# CHAPTER 4

# ACCELERATOR AND DETECTOR

Stretching 27 km in circumference as it straddles the Switzerland-France border near Geneva, Switzerland, CERN's Large Hadron Collider (LHC) is the largest and most powerful particle accelerator in the world; the LHC is described in detail in [16], which will be summarized in section 4.1. Within the LHC, two counterrotating beams of protons are accelerated to a center of mass energy of 13 TeV before being made to collide within the four main particle detectors at the LHC. One of the two general-purpose detectors at the LHC, the Compact Muon Solenoid (CMS) detector is designed to measure and to record the energies, charges, and momenta of the particles produced by the high-energy collisions. A detailed description of the CMS detector is provided in [17], which will be summarized in section 4.2.

## 4.1 The large hadron collider

Before being injected into the LHC, the proton beams are accelerated by a series of smaller machines in the LHC accelerator complex. The beams enter the LHC with an energy of 450GeV. Superconducting dipole magnets steer the beams around the ring. With a "twin-bore" design, the clockwise and counterclockwise beams are guided by separate coils of magnets in separate beam channels that reside in the same beampipe. Each beam is accelerated to a final energy of 6.5 TeV (during the 2016-2018 data-taking periods) by radio frequency (RF) cavities [18]. The RF cavities also help to keep the protons separated into discrete groups referred to as bunches. There are about $10^{11}$ protons in each bunch, and the machine can be filled with a

maximum of 2808 bunches. The nominal bunch spacing is 25 ns, meaning that the collision rate (i.e. bunch crossing rate) is about 40 MHz.

## 4.2 The CMS detector

The CMS detector is composed of multiple concentric subdetectors, each designed to measure the properties of different types of particles produced in the collisions. Cylindrical in shape, the detector has a length of 21.6 m, a diameter of 14.6 m, and a weight of 12,500 t. The coordinate system used by CMS is explained in Section 4.2.1. A schematic of the CMS detector (illustrating the various subdetectors) is shown in Figure 4.1.

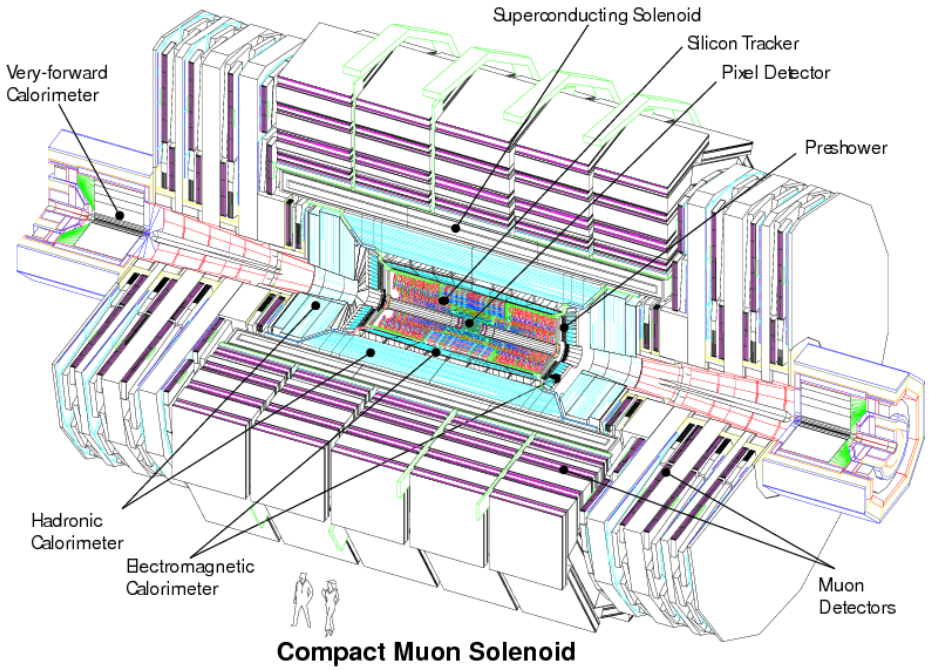


Figure 4.1. Schematic of the CMS detector with the main subdetectors labeled. [17]

The innermost subdetector is the tracker; it is composed of silicon and is responsible for recording the trajectories of the charged particles that emerge from the collisions. The tracker is discussed in Section 4.2.2. Surrounding the tracker, the electromagnetic calorimeter (ECAL) is a homogenous calorimeter that measures the energy of electrons and photons by detecting the scintillated light produced as the particles shower in the lead tungstate crystals that compose the ECAL. The ECAL is described in Section 4.2.3. The hadronic calorimeter (HCAL) surrounds the ECAL. Responsible for measuring the energies of charged and neutral hadrons, the HCAL is a sampling calorimeter composed of layers of brass absorber and plastic scintillator. The HCAL is discussed in Section 4.2.4. Beyond the HCAL lies CMS's superconducting solenoid magnet. With a magnetic field of 3.8 T, the solenoid bends the paths of charged particles as they traverse the detector, allowing their charge and momentum to be determined. Outside of the solenoid magnet are the CMS muon systems; composed of gas ionization detectors, the CMS muon system records the paths of muons as they pass through the detector. The muon detectors are described in Section 4.2.5. Responsible for parsing information from each subdetector in order to determine which collision events to record and which to reject, the CMS trigger system is described in Section 4.2.6.

### 4.2.1 Coordinate system

This section will summarize the coordinates and conventions used by the CMS experiment, which are illustrated in Figure 4.2. The origin of the coordinate system is the nominal interaction point inside the CMS detector. The $x$ axis points radially inward toward the center of the LHC accelerator, the $y$ axis points upward, and the $z$ axis points along the beam line in the counterclockwise direction. The azimuthal angle $\phi$ is measured from the $x$ axis in the $x-y$ plane, and the polar angle $\theta$ is measured from the $z$ axis in the $z-y$ plane.

The rapidity is defined as $\frac{1}{2}\ln\left(\frac{E+p_z}{E-p_z}\right)$. Differences in rapidity are preserved under boosts along the $z$ direction, so the relative rapidity between particles is meaningful even if the particles have different boosts. Similarly, the pseudorapidity is defined as $\eta = \frac{1}{2}\ln\left(\frac{|\vec{p}|+p_z}{|\vec{p}|-p_z}\right) = -\ln\tan\left(\frac{\theta}{2}\right)$. Thus $\eta$ is zero along the $y$ axis and $\eta$ approaches infinity along the beam line. In the limit that $|\vec{p}| \gg m$ (a good approximation for stable particles produced at the LHC), the rapidity and pseudorapidity are equal, so the pseudorapidity is usually used to describe angles in the $z-y$ plane.

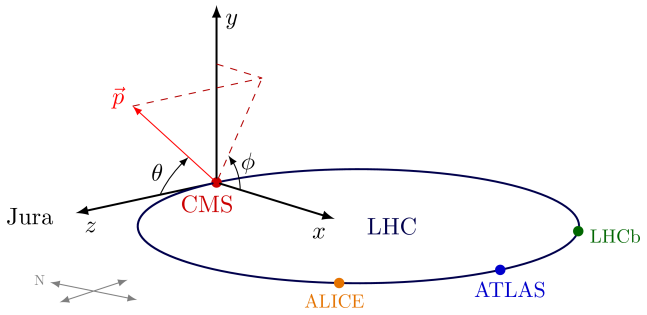


Figure 4.2. Coordinates used by the CMS experiment. An example momentum vector $\vec{p}$ is shown. [19]

Since the total momentum in the $z$ direction varies for each collision, it is useful to consider the momentum in the plane transverse to the beam (the $x-y$ plane), where the total momentum of the colliding partons is zero. We thus define the transverse momentum $p_T = |\vec{p}|\sin(\theta) = \sqrt{p_x^2 + p_y^2}$. Conservation of momentum requires that the sum of the transverse momentum vectors of the particles produced in the collision must be zero, so momentum that is carried away by neutrinos (or by any other hypothetical particles that are invisible to CMS) can be identified as the opposite of the sum of the $p_T$ vectors of all of the visible particles produced in the collision; the magnitude of this vector is referred to as the missing transverse momentum, or $p_{\mathrm{T}}^{\mathrm{miss}}$.

### 4.2.2 The inner tracker

The CMS inner tracker is described in detail in Refs. [17, 20, 21]. The purpose of the tracker is to record the trajectories of charged particles without significantly disturbing their momenta. Since the tracker is the innermost component of the detector and is thus closest interaction point, it must have fine granularity yet be able to withstand high levels of radiation. Silicon provides these characteristics, so this is the material that was chosen for the CMS tracker. The tracker comprises two concentric subdetectors. Referred to as the silicon pixel detector and the silicon strip detector, these subdetectors are illustrated in in Figure 4.3.

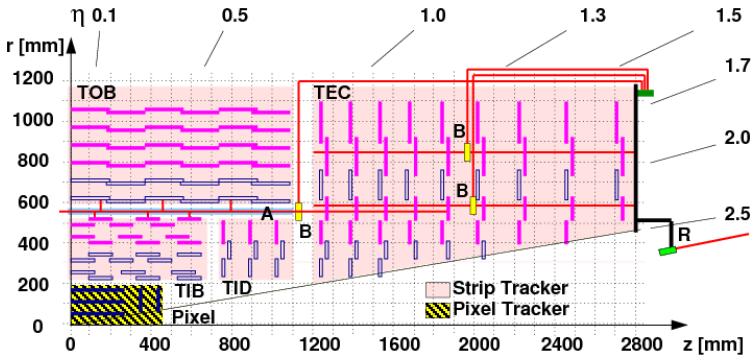


Figure 4.3. Diagram of a quadrant of the CMS tracker showing the pixel and strip trackers (with the interaction point at the lower lefthand corner of the schematic). [22]

Closest to the interaction point, the pixel detector contains 66 million silicon sensors referred to as pixels. Each pixel is 100$\mu$m by 150$\mu$m, so the total surface area of the pixel detector is about 1m$^2$. In the barrel region the pixel detector has several layers of sensors; the innermost layer has a radius of about 4cm, and the outermost layer has a radius of about 11cm. The endcaps have two layers of sensors, extending the coverage of the pixel detector over a range of $|\eta| < 2.5$. Surrounding the pixel

detector is the silicon strip detector. Composed of 9.6 million silicon sensors, this detector comprises 10 layers in the barrel and 12 layers in each end cap. The silicon strip detector has a length of 5.8 and a diameter of 2.5m, and the total surface area of its sensors is about $200\text{m}^2$ (i.e. about the area of a singles tennis court).

The pixel tracker and the strip tracker record the paths of charged particles through the same mechanism. Silicon is a semiconductor, and its properties can be manipulated to provide sensitive detection of ionizing particles. Through the process of doping, n-type semiconductors (with excess electrons) and p-type semiconductors (with missing electrons i.e. holes) may be constructed from silicon. Interfacing p-type silicon with n-type silicon, a p-n junction is created. When an electric potential is applied such that the positive terminal is connected to the n-type region and the negative terminal is connected to the p-type region, the mobile charge carriers (electrons and holes) will move towards the positive and negative terminals, causing the region at the interface to become depleted of mobile charge. This arrangement is referred to as a reverse biased junction. An incoming particle may then ionize silicon atoms as it traverses the p-n junction in a pixel or strip sensor, resulting in free electrons that will move towards the positive terminal, producing a small pulse of current that can be amplified and recorded. This signal is referred to as a "hit" in the tracker. The hits are linked together to determine the path of the charged particle through the detector.

### 4.2.3 The electromagnetic calorimeter

The CMS ECAL is described in detail in Refs. [17, 20, 23]. The purpose of the ECAL is to measure precisely the energy of electrons and photons, absorbing the particles in the process. Constructed of lead tungstate ($PbWO_4$) crystals, the ECAL is a homogenous detector, which provides good energy resolution, as the entire detector is composed of active medium.

Lead tungstate has a high density and a short radiation length (a characteristic of the material corresponding to the mean distance an electron travels before losing all but $1/e$ of its energy via bremsstrahlung), allowing for a relatively compact design. The Molière radius (the radius in which approximately 90% of a shower energy is contained, a characteristic that is related to the radiation length) is correspondingly small, providing fine granularity and less overlap between the energy deposits of different particles. Figure 4.4 illustrates the components of the ECAL.

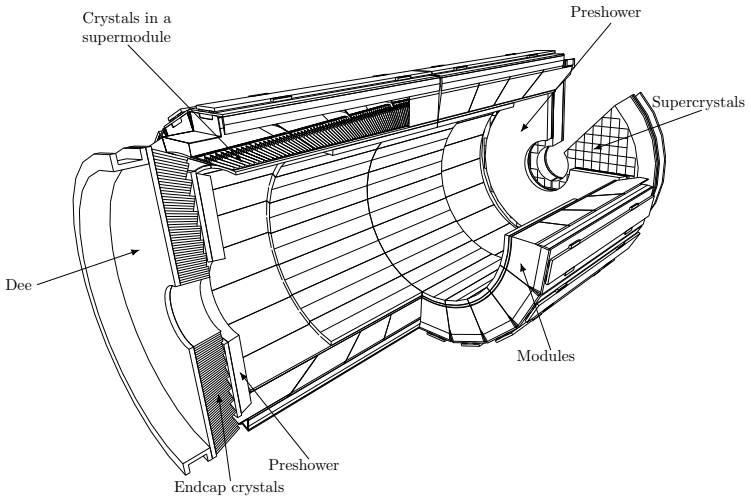


Figure 4.4. Diagram of the CMS ECAL, with components labeled. [17]

The barrel region of the ECAL contains over 60k crystals and covers a range of $|\eta| < 1.479$. The ECAL endcaps contain over 12k crystals and cover the $1.479 < |\eta| < 3.0$ regions. Spanning about 25 radiation lengths, the ECAL is able to contain more than 98% of the energy of the incoming electrons and photons. Incoming particles interact electromagnetically with the ECAL crystals, producing light in proportion to their energy. A photodetector is attached to each crystal to collect the scintillated

light; avalance photodiods are used for the barrel, while vacuum phototriods are used in the endcaps.

In front of each endcap, a finer-grained detector (referred to as the preshower detector) helps to identify pairs of photons arising from $\pi^0$ decays. With a total width of about 20cm, the preshower detector is a sampling calorimeter composed of lead and silicon; the lead layer initiates the electromagnetic shower, while the slicon sensors measure the energy of the shower. The preshower detector covers a range of $1.653 < |\eta| < 2.6$.

### 4.2.4 The hadronic calorimeter

The CMS HCAL is described in detail in Refs. [17, 20, 24]. Composed of layers of brass absorber and plastic scintillator material, the HCAL is a sampling calorimeter designed to measure the energy of hadrons, absorbing them in the process. The HCAL has several subcomponents covering the barrel and endcap regions, as illustrated in Figure 4.5.

Constrained to fit between the outer radius of the ECAL (at 1.77m) and the inner radius of the solenoid magnet (2.95m), the main barrel region of the HCAL (HB) covers the range of $|\eta| < 3.0$. The total depth of the HB absorber is about six interaction lengths (where the interaction is the average length traveled by a particle before undergoing an interaction with the material). In the barrel region outside of the solenoid magnet, the HB is aided by an additional HCAL layer known as the outer detector (HO), which extends the total depth of the calorimeters to about 12 interaction lengths (this includes the $\sim$1 interaction length provided by the ECAL material). On the endcaps, the HCAL endcaps detectors (HE) cover the range of $1.3 < |\eta| < 3.0$ with a depth of about 10 interaction lengths (including the ECAL material). Like the barrel detector, the HE is composed of brass absorber and plastic scintillator.

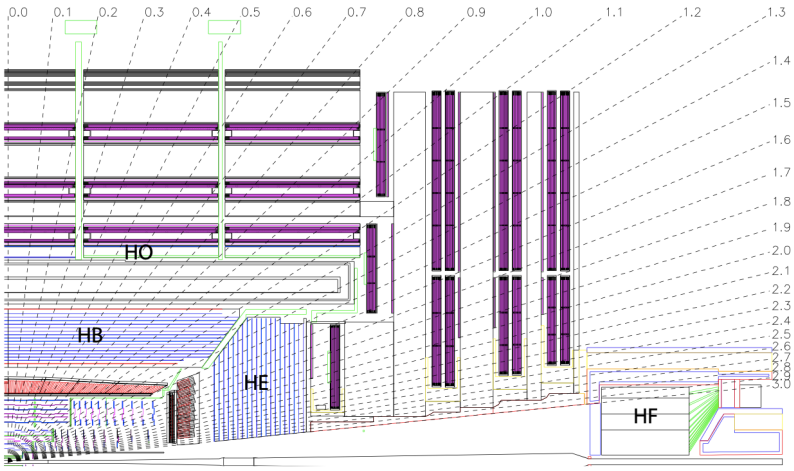


Figure 4.5. A quadrant of the CMS HCAL (with the interaction point at the lower lefthand corner). The barrel detector (HB), outer barrel detector (HO), endcap detector (HE), and forward detector (HF) are shown. [17]

To extend the $\eta$ coverage of the HCAL to an $|\eta|$ of 5, a forward component (HF) is positioned beyond the muon systems as shown in Figure 4.5. Due to the high particle flux in the forward region, the design of the HF prioritizes radiation hardness. For this reason, quartz fibers were chosen as the active material. The HF detector is composed of steel absorber with grooves in which the quartz fibers are inserted. Signal in the HF is produced when shower particles generate Cherenkov radiation in the quartz fibers.

### 4.2.5 The muon detectors

The CMS muon detectors are described in detail in Refs. [17, 20, 25]. The purpose of the system is to identify muons, accurately reconstructing their momenta and charges. Composed of three subdetectors, the muon systems identify muons through the same basic mechanism; as muons pass through gaseous chambers, they ionize the gas and the free electrons drift towards positively charged wires or plates, creating signals known as hits. The muon detectors are illustrated in Figure 4.6.

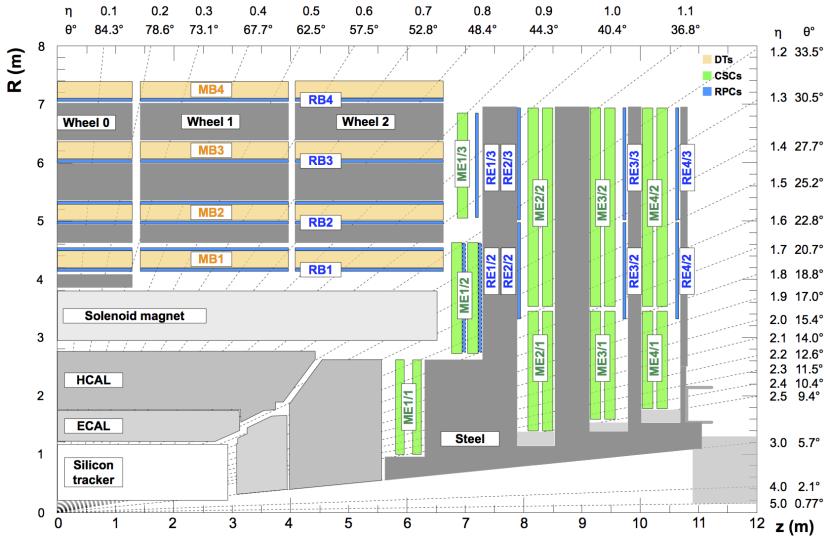


Figure 4.6. Diagram of a quadrant of the CMS detector (with the interaction point at the lower lefthand corner) illustrating the muon chambers. The components labeled "MB" represent the DTs, the components labeled "ME" represent the CSCs, and the components labeled "RE" and "RB" represent the RPCs. [25]

In the barrel region, 250 drift tube chambers (DTs) cover the $|\eta| < 1.2$ range. Each DT is filled with a mixture of Ar and $CO_2$ and contains a positively charged wire running through the chamber. When muons ionize the gas, the electrons drift towards the positively charged wire, producing a signal that is recorded as a hit. The location of the muon in the DT the chamber can be determined based the observed drift time and the known drift velocity.

In the endcaps, over 500 cathode strip chambers (CSCs) cover a range of $0.9 < |\eta| < 2.4$. The CSCs are finely segmented, with negatively charged cathode strips running radially outward (towards which the positive ions drift) and positively charged wires running approximately perpendicularly to the strips (towards which the electrons drift). This high resolution is important for the CSCs, as the endcaps are subject to high muon fluxes and a non-uniform magnetic field.

In both the barrel and endcap regions, about 1000 additional detectors known as

resistive plate chambers (RPCs) cover a range of $\eta < 1.9$. Unlike the DTs and CSCs, the RPCs do not contain wire anodes. Rather, positively and negatively charged parallel plates lining the chamber form the anode and cathode for the detector. The RPCs provide fine timing resolution, but coarse position resolution; the precision timing information is useful for the muon triggers.

### 4.2.6 The trigger systems

Bunch crossings take place within CMS at 40 MHz, producing data at about 40 TB/s. This is much more data than could be recorded or stored for future analysis; however, only a small fraction of these collisions contain events likely to be associated with new or interesting phenomena. In order to select as many of the potentially interesting events as possible while reducing the rate to a more manageable 1 kHz, CMS employs a two-tiered trigger system consisting of a hardware based Level-1 (L1) trigger [26] and a software based high level trigger (HLT).

The L1 trigger is responsible for reducing the rate to approximately 100 kHz. Since collisions take place at 40 MHz, the L1 trigger must on average make a decision every 25 ns. The detector is capable of buffering data from 160 collisions [27], so the L1 trigger is able to have a latency of $4\mu s$; however, this is not enough time for the data from the tracker to be reconstructed, so the L1 trigger uses information from only the calorimeters and the muon detectors.

Figure 4.7 shows a schematic of the L1 trigger system architecture. As shown in the figure, the data from the calorimeters are received by the Layer 1 Calorimeter Trigger; these data corresponds to the energy deposits recorded by the calorimeters and are referred to as trigger primitives (TPs). The Layer 2 Calorimeter Trigger reconstructs physics objects from the TPs, and the demultiplexer board ("DeMux") serializes and formats the events to be sent to the L1 Global Trigger. From the muon systems, the muon track finder (MTF) algorithms combine information from

the DTs, CSCs, and RPCs, using the concentrator and preprocessor fanout (CPPF) to cluster hits from the endcap RPCs into TPs and the TwinMux [28] to combine information from the DTs and RPCs. The MTFs pass the candidate objects to the Global Muon Trigger, which selects up to 8 objects to pass to the L1 Global Trigger.

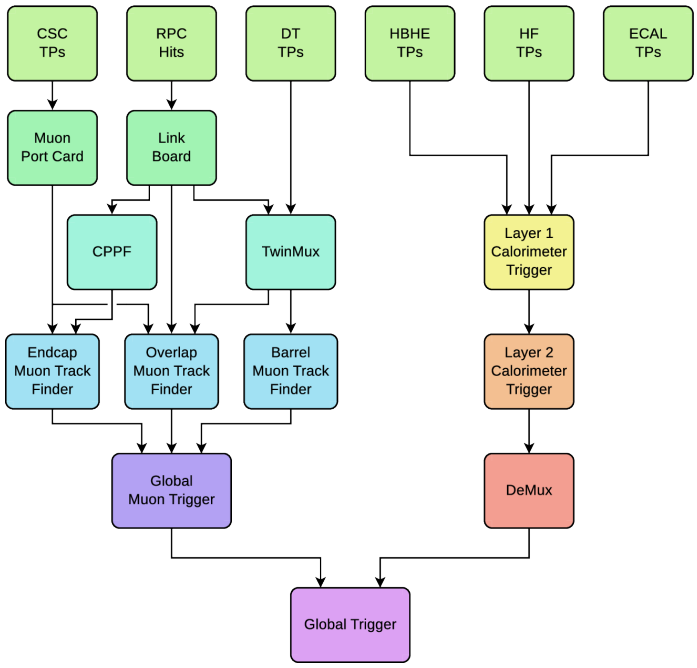


Figure 4.7. Schematic of the L1 trigger system, as described in the text. [26]

The L1 Global Trigger receives the calorimeter and muon objects and executes a set of algorithms on these objects; the algorithms are designed to identify events involving potentially interesting phenomena, e.g. events with multiple muons or events with high $p_T$ jets. The set of algorithms is referred to as the L1 trigger menu, and the total number of algorithms in the menu is typically about 400. If an event passes the selection criteria for any of the algorithms in the menu, the L1 Global Trigger accepts the event. The event is otherwise discarded.

If the L1 Global Trigger accepts an event, the data acquisition system reads out all of the data associated with the event and sends the data to the HLT. The HLT consists of a farm of processors comprising approximately 30,000 CPU cores. Responsible for reducing the rate of accepted events to about 1 kHz, the HLT has a latency of about 300 ms. This latency allows the HLT to execute sophisticated reconstruction algorithms that are similar to offline reconstruction, using information from all of the subdetectors including the tracker. The HLT uses a simplified version of the particle flow (PF) reconstruction algorithm used for offline reconstruction (described in Chapter 5). Optimized for CPU speed, the online reconstruction does not incorporate electron identification into PF, and does not perform reconstruction for low $p_T$ tracks in the inner tracker [20].

Similar to the L1 menu, the HLT menu consists of a set of selection criteria targeting potentially interesting signatures. The reconstruction steps are performed in a set order, with faster steps being executed first and slower steps executed last. This ordering allows events that do not pass the selection criteria for any of the paths in the menu to be rejected as quickly as possible. If an event passes the selection requirements for any of the algorithms in the HLT menu, it is transferred to the CMS Tier-0 computing center to be processed offline and stored permanently.